Microtubule Sliding in Mutant *Chlamydomonas* Axonemes Devoid of Outer or Inner Dynein Arms

Tsuyoshi Okagaki and Ritsu Kamiya

Institute of Molecular Biology, Faculty of Science, Nagoya University, Nagoya, 464 Japan. Dr. Okagaki's present address is the Physics Science Laboratories, Nihon University at Narashino, Narashino-dai, Funabashi, Chiba, 274 Japan.

Abstract. To clarify the functional differentiation between the outer and inner dynein arms in eukaryotic flagella, their mechanochemical properties were assessed by measuring the sliding velocities of outer-doublet microtubules in disintegrating axonemes of *Chlamydomonas*, using wild-type and mutant strains that lack either of the arms. A special procedure was developed to induce sliding disintegration in *Chlamydomonas* axonemes which is difficult to achieve by ordinary methods. The flagella were first fragmented by sonication, demembranated by Nonidet P-40, and then perfused under a microscope with Mg-ATP and nagarse, a bacterial protease with broad substrate specificity. The sliding velocity varied with the Mg-ATP concentration in a Michaelis-Menten manner in the axonemes from the wild type and a motile mutant lacking the outer dynein arm (*oda38*). The maximal sliding velocity and apparent Michaelis constant for Mg-ATP were measured to be 13.2 ± 1.0 μm/s and 158 ± 36 μM for the wild type and 2.0 ± 0.1 μm/s and 64 ± 18 μM for *oda38*. These maximal sliding velocities were significantly smaller than those estimated in beating axonemes; the reason is not clear. The velocities in the presence or absence of 10^{-5} M Ca^{2+} did not differ noticeably. The axonemes of nonmotile mutants lacking either outer arms (*pf13A*, *pf22*) or inner arms (*pf23*) were examined for their ability to undergo sliding disintegration in the presence of 0.1 mM Mg-ATP. Whereas *pf13A* axonemes underwent normal sliding disintegration, the other two species displayed it only very poorly. The poor ability of *pf23* axonemes to undergo sliding disintegration raises the possibility that the outer dynein arm cannot function well in the absence of the inner arm.

THE inner and outer dynein arms in eukaryotic flagella and cilia differ completely in protein composition (14, 25, 26) and morphology (1, 9, 10, 34) and thus may differ in function, although no clear evidence for this has been reported. Studies using procedures to selectively extract the outer arm (8, 37) or observations on mutant flagella lacking it (18, 22) have indicated that axonemes lacking outer dynein arms display reduced beat frequency but not total lack of motility. Hence the outer arm is not absolutely necessary for axonemal beating. However, no conclusive findings have yet been reported as to whether or not the inner arm is dispensable. One unique *Chlamydomonas* mutant that lacks the inner arm (*pf23*; reference 14) is nonmotile, but this cannot be taken as evidence for its absolute necessity; further studies may reveal the existence of motile mutants lacking the inner arm.

To assess the mechanochemical property of the inner and outer dynein arms, we measured the sliding velocity of microtubules extruded from wild-type and mutant axonemes of *Chlamydomonas*, upon perfusion with a protease and ATP. Since the first report by Summers and Gibbons in 1971 (29), active sliding of outer doublet microtubules in protease-treated axonemes has been demonstrated in cilia and flagella of a wide variety of cells (7, 16, 20, 23, 27, 28, 32, 35, 38). By recording the dynamic process of the disintegration, several authors have measured the sliding velocity of microtubules under various conditions and thereby examined the effect of ATP concentration (12, 31, 39), Ca^{2+} concentration (23), or removal of the outer dynein arm (13, 40) on this mechanochemical process. The measurement of sliding velocity, as a method to estimate the mechanochemical properties of dynein–microtubule systems, is simpler than analysis of axonemal beating and has the advantage of being applicable to mutant axonemes that do not beat; the possibility that protease-treated axonemes from paralyzed flagella mutants of *Chlamydomonas* undergo the sliding disintegration has been demonstrated by Witman et al. with mutants lacking the central pair or radial spoke systems (38). However, as observation of microtubule sliding in *Chlamydomonas* axonemes was much more difficult than in axonemes from other sources, such as *Tetrahymena* or sea urchin sperm, we first established an experimental procedure to efficiently cause the sliding disintegration. With our improved method, we were able to obtain reproducible values for the sliding velocity under given sets of conditions. We report here the results with mutant axonemes lacking outer or inner arms, as well as those with the wild-type axonemes.

Materials and Methods

Culture of Cells

Chlamydomonas reinhardtii 137c mt+ (wild type), *oda38* (18), *pf13A* (14), *pf22* (14), and *pf23* (14) were used. All the *pf* mutants were kindly supplied by Dr. David Luck (The Rockefeller University, NY). Wild-type and *oda38* cells were grown in Tris-acetic acid-phosphate (TAP) medium (11) and *pf* mutants on 1.5% agar plates containing TAP medium under continuous illumination. Each strain was cultured either in 2 liters of liquid medium or on 150 ml of agar medium in five 9-cm Petri dishes. Cells grown on the agar plates were scraped off and suspended in nitrogen-free medium (21) to induce formation of flagellated gametes, after 1 wk of culture.

Preparation of Axonemes

Flagella were detached from the cell body by using dibucaine and isolated by centrifugation, as described by Witman et al. (38). The suspension of flagella was sonicated in a Kubota 200M sonicator (Kubota Co., Tokyo) at a setting of 20 W for ~50–80 s so that the length of the axoneme became about half the original value on the average. The fragmented axonemes were sedimented by centrifugation at 10,000 *g* for 20 min and demembranated by suspending the pellet in an ice-chilled solution containing 10 mM Hepes (pH 7.4), 5 mM $MgCl_2$, 1 mM dithiothreitol (DTT), 1 mM EGTA, 0.5% polyethylene glycol (20,000 mol wt), 30% glycerol, and 0.3% Nonidet P-40. The protein concentration of this suspension was adjusted between 0.5 and 1 mg/ml.

Observation of Microtubule Sliding

A small volume of the suspension of fragmented axonemes was mixed with ~10 vol of a reactivation solution containing 10 mM Hepes (pH 7.4), 5 mM $MgCl_2$, 1 mM DTT, 1 mM EGTA, 0.5% polyethylene glycol, and an appropriate concentration of ATP to give the desired concentration of Mg-ATP (for example, 1.04 mM for the reactivation solution of 1.00 mM Mg-ATP). When the effect of Ca^{2+} was examined, 1 mM EGTA was replaced by 2 mM EDTA and 0.5 mM $CaCl_2$; the calcium ion concentration of this solution was calculated to be $\sim 1 \times 10^{-5}$ M, regardless of the Mg-ATP concentration up to 1 mM. A drop of the sample was placed on a glass slide and covered with a coverslip. Two opposite sides of the coverslip were sealed with Vaseline while the other two sides were left open. This specimen was perfused with the same reactivation solution containing 0.5 μg/ml nagarse (Type VII bacterial protease; Sigma Chemical Co., St. Louis, MO), by placing a drop of perfusion solution and a filter paper tip by the two opposite, unsealed sides of the coverslip. Sliding disintegration of the axonemes usually took place within a few minutes after the perfusion was started. The process of disintegration was observed with a dark-field microscope equipped with a 40× oil-immersion objective and a light source of a 100-W high-pressure mercury arc lamp, and recorded on videotape with an SIT camera (17). Observations were made at 23 ± 1°C.

Measurement of Sliding Velocity

Videotapes of the sliding microtubules were played back frame-by-frame on a monitor using the "stop-motion" mode of a videotape recorder. The position of the tip of moving microtubule was marked every 1/10 to 1/5 s on a transparent sheet overlaid on the monitor screen, and its distance from the original position was plotted against time. When a microtubule is sliding uniformly, this plot should display a linear increase with time. We drew a linear regression line where more than five data points showed reasonable linearity and obtained the velocity from its slope. Under a given set of conditions, we took data from at least 15 scenes and averaged them to obtain the final value of the velocity. When there was any possibility that two or more microtubules were sliding simultaneously, the data was not included because such a multiple sliding event would cause the tip to move faster than the real sliding velocity between two microtubules.

Other Methods

The percentage of axoneme fragments that underwent sliding disintegration was estimated by counting under the microscope the number of axoneme fragments that clearly appeared to have disintegrated by sliding (*A*) or by fraying into bundles of microtubules (*B*), and that of axoneme fragments that did not appear to have disintegrated at all (*C*), after a sufficiently long period of perfusion. Free microtubules or bundles of microtubules apparently thinner than axonemes were not counted. We estimated the frequency of sliding disintegration by the ratio $A/(A + B + C)$. The estimation was difficult and not reliable when axonemes tended to disintegrate extensively into thin bundles of microtubules, as when the Mg-ATP concentration was <50 μM. The frequency of occurrence of sliding disintegration we experienced while recording the image was usually much lower than the one estimated by the above method. This low frequency was possibly due to an inhibitory effect of the intense light on the sliding.

Protein concentrations of axoneme samples were determined by the method of Bradford (4). In a survey of proteases, trypsin (Type I; Sigma Chemical Co.) and elastase (Type II; Sigma Chemical Co.) were used.

Results

Efficient Induction of Microtubule Sliding

It was difficult to observe the microtubule sliding process in isolated axonemes of wild-type *Chlamydomonas*. In the reactivation solution, 20–40% of the axonemes were observed to beat with an asymmetric waveform (3). When perfused with proteases in the presence of ATP, most of these axonemes stopped beating and disintegrated by fraying into bundles of doublet microtubules with the basal portion bound together, as observed by Witman et al. (38) (Fig. 1, *a* and *b*; Table I). Apparently the difficulty with *Chlamydomonas* axonemes arose from the presence of a basal portion resistant to proteolysis. We therefore fragmented the flagella by sonication treatment, before demembranation, to produce axoneme pieces free of the basal part. The sonication treatment reduced the average length of axonemes to about half that of the intact axonemes; the average lengths of the intact and sonicated axonemes in one sample were 11.5 ± 1.6 μm and 5.3 ± 1.6 μm, respectively. The fragmented axonemes underwent sliding disintegration much more frequently than the intact axonemes upon perfusion with ATP and protease (Fig. 1, *c–f*; Table I).

To further improve the conditions for inducing sliding disintegration, we tested three kinds of proteases (trypsin [29], elastase [5], and nagarse) for their ability to cause it in sonicated axonemes. All were included in the perfusing solution at various concentrations between 0.2 and 4 μg/ml, and the percentage of the axonemal fragments that underwent sliding disintegration was measured at 0.1 mM Mg-ATP. We found that the protease concentration for efficient induction of sliding disintegration must be ≥2 μg/ml with trypsin, 1.5 μg/ml with elastase, and 0.5 μg/ml with nagarse. The percentage of axonemes that underwent sliding disintegration and the sliding velocity of microtubules measured in a typical experiment using these three kinds of proteases are shown in Table I. As the results indicated that nagarse, a protease with a rather broad specificity (2), would give the best results in terms of efficiency and velocity of the sliding disintegration, we used 0.5 μg/ml nagarse in all of the following experiments.

Effect of ATP Concentrations on the Sliding Profiles

Fig. 1, *c* and *d*, and Fig. 1, *e* and *f*, show fragments of wild-type axonemes before and after perfusion with protease solutions containing 1 mM (*c* and *d*) and 20 μM (*e* and *f*) Mg-ATP. At the higher Mg-ATP concentration, the axonemes tended to extrude groups of microtubules at once, possibly because sliding took place only between one or two pairs of microtubules. Further disintegration of the microtu-

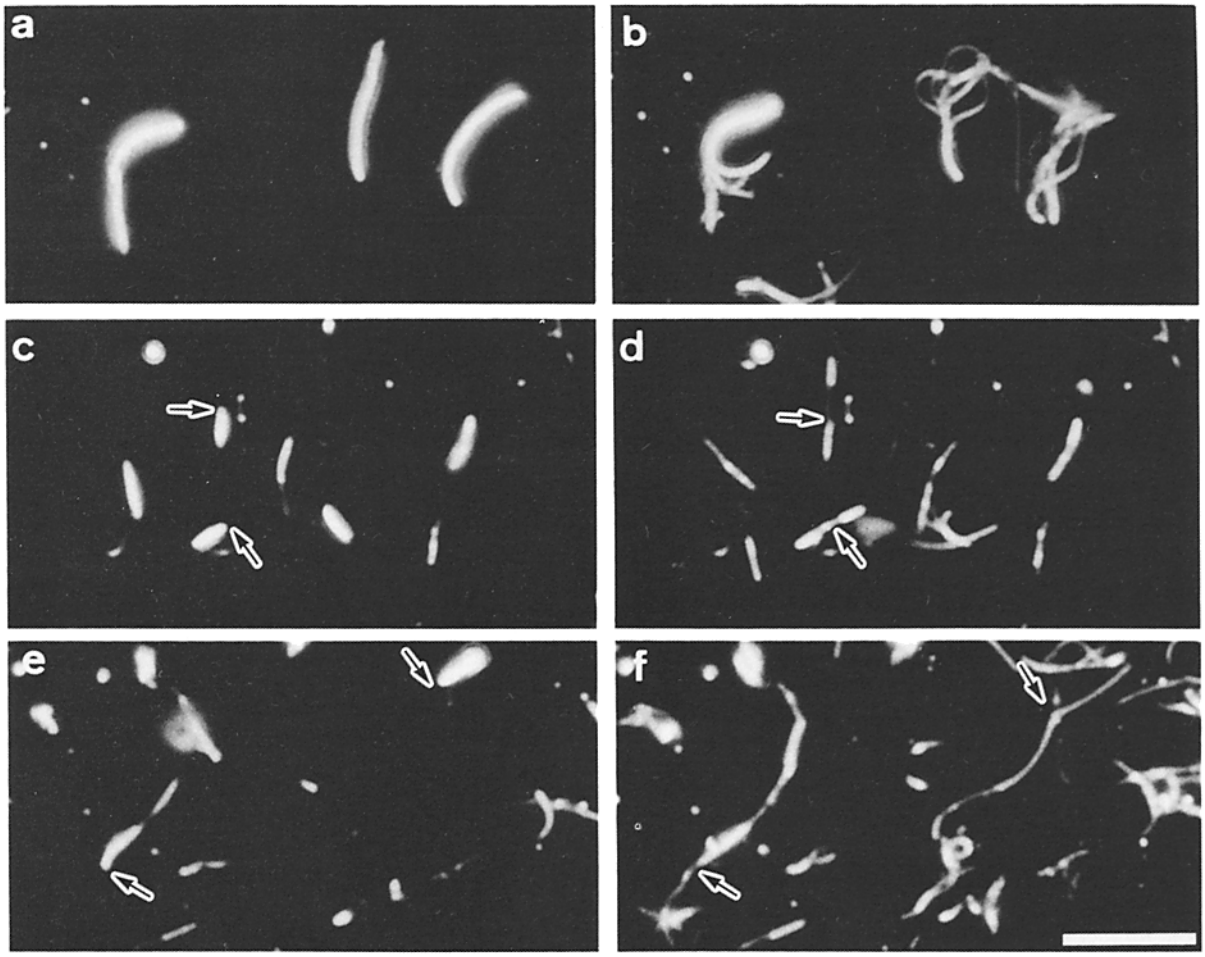

Figure 1. Disintegration of wild-type axonemes upon perfusion with nagarse and Mg-ATP. (*a* and *b*) Intact axonemes before (*a*) and after (*b*) disintegration in 1 mM Mg-ATP; (*c* and *d*) sonicated axonemes disintegrating in 1 mM Mg-ATP; (*e* and *f*) sonicated axonemes disintegrating in 0.02 mM Mg-ATP. Arrows indicate tips of axoneme fragments that undergo sliding. Dark-field micrographs. Bar, 10 μm.

bule bundles did not occur under our experimental conditions. At the lower Mg-ATP concentration, however, sliding appeared to occur between several pairs of microtubules and, as a result, the final length of the microtubule chains became longer than those observed at higher Mg-ATP concentrations. The plot of the final length of disintegrated axonemes and the Mg-ATP concentration showed a clear inverse relationship (Fig. 2). The reason for this is not understood at present, but may be related to the phenomena observed in *Tetrahymena* axonemes; sliding disintegration of axonemes without protease treatment has been reported to be inhibited by Mg-ATP concentrations higher than ~20 μM (30, 36).

Table I. Sliding Disintegration with Different Proteases

	None*	Trypsin	Elastase	Nagarse
Intact axonemes				
Disintegrated				
by sliding (%)	1	12	23	36
by fraying (%)	6	81	66	57
Not disintegrated (%)	93	7	11	7
Sonicated axonemes				
Disintegrated				
by sliding (%)	17	56	63	70
by fraying (%)	4	26	19	21
Not disintegrated (%)	79	18	18	9
Sliding velocity (μm/s)		4.7 ± 0.7 (n = 10)	6.0 ± 1.2 (n = 13)	6.5 ± 1.5 (n = 17)

* No protease was added to the perfusion solution. Concentrations of proteases used were 2 μg/ml (trypsin), 1.5 μg/ml (elastase), and 0.5 μg/ml (nagarse). Mg-ATP concentration: 0.1 mM. More than 500 axonemes were counted for each estimation of the percentage of disintegrated axonemes.

ATP-dependent Sliding Velocities in Wild-Type and Outer-Armless Axonemes

The process of sliding disintegration could be observed and recorded with a sensitive video system. Fig. 3 shows videotape sequences of axoneme fragments disintegrating in the presence of 1 mM (*a*) and 20 μM Mg-ATP (*b*). In Fig. 3 *a*, the sliding disintegration took place in a discontinuous manner, with elongating and resting phases. Each elongating phase appears to occur due to a sliding between one pair of microtubules, as judged by the length increase and the change in the image intensity of each sliding block during this phase. In contrast, the axoneme fragment in Fig. 3 *b* elongated smoothly until its length reached about four times the original value. In this case, several pairs of microtubules must have been simultaneously undergoing sliding disin-

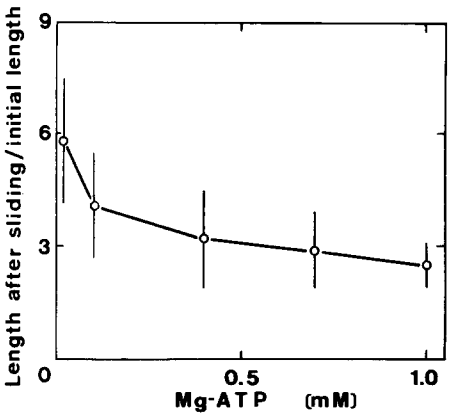

Figure 2. Increase in the end-to-end length of wild-type axoneme fragments after completion of sliding disintegration at different concentrations of Mg-ATP. These data are average values from ~20 measurements at each Mg-ATP concentration. At any Mg-ATP concentration, 20–30% of the axoneme fragments did not undergo sliding disintegration at all. Such axonemes were not counted here.

tegration and the tip of the bundle moving much faster than the real sliding velocity between two microtubules.

We measured the sliding velocity of outer-doublet microtubules from those images which were judged as representing a sliding between one pair of microtubules, as in an elongating phase in Fig. 3 *a*, by plotting the distance of the moving tip from its original position against time. Examples of such a plot for wild-type axonemes disintegrating at different ATP concentrations are shown in Fig. 4. As noted in previous studies with other kinds of axonemes (31, 39), the sliding velocity was dependent on the Mg-ATP concentration and fairly uniform just until the sliding stopped. The measured values of velocity varied by as much as ± 25% under a given set of conditions but the variation did not appear to be correlated with the length of the axonemal fragments (data not shown).

Axoneme fragments from *oda38*, a motile mutant lacking the outer dynein arm (18), were also found to display sliding disintegration, although the velocity was much smaller than in the wild type (Fig. 6, *a* and *b*). In both wild-type and *oda38* axonemes, the sliding velocity varied with the Mg-ATP concentration in a Michaelis-Menten manner. Fig. 5 shows the double reciprocal plot of the data obtained with three different preparations of wild-type and *oda38* axonemes. Although there is considerable scatter of the data, especially in the *oda38* axoneme, these plots show a reproducible, straight relationship for both species. The maximal sliding velocity and the apparent Michaelis constant for the two kinds of axonemes, averaged from three sets of experiments for each, were 13.2 ± 1.0 μm/s and 158 ± 36 μM (wild-type) and 2.0 ± 0.1 μm/s and 64 ± 18 μM (*oda38*). The maximal sliding velocity thus measured in wild-type *Chlamydomonas* is slightly smaller than that of sea urchin sperm microtubules, of which 14–19 μm/s has been reported as the maximal velocity (31, 39).

Effect of Ca^{2+}

The beating pattern of *Chlamydomonas* axonemes is regulated by Ca^{2+} (3, 15, 19, 24). Wild-type axonemes beat with a ciliary pattern at Ca^{2+} concentrations lower than 10^{-6} M, but with a flagellar pattern at higher concentrations (3, 15). The *oda38* axonemes do not beat at Ca^{2+} concentrations higher than 10^{-6} M (18). To find whether Ca^{2+} has any effect on the sliding disintegration of axonemes, we measured the sliding velocity in the presence and absence of 10^{-5} M Ca^{2+}

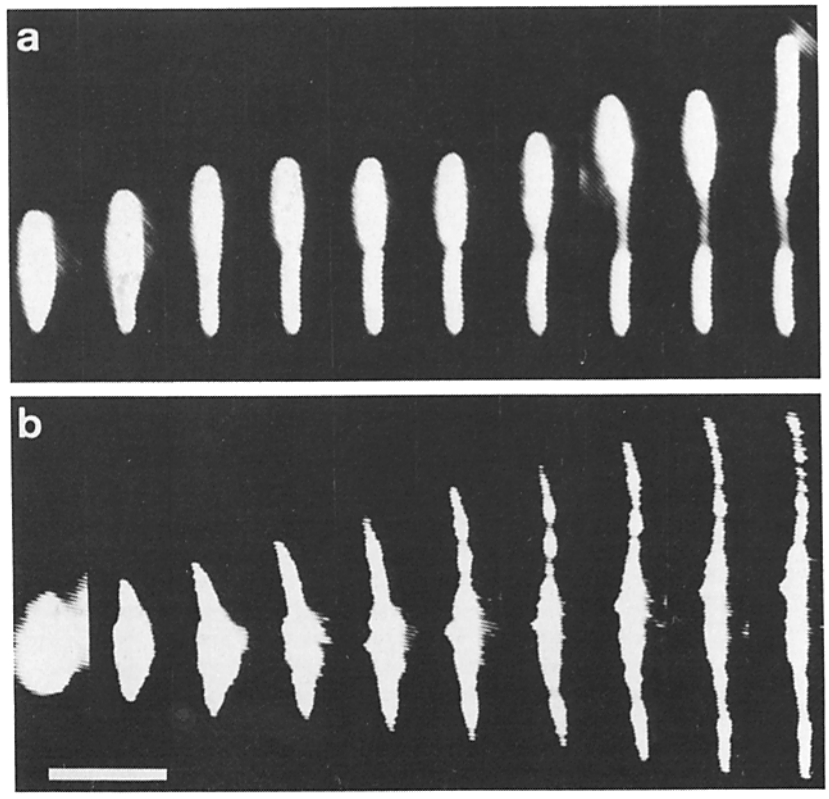

Figure 3. Videotaped sequences of wild-type axonemes undergoing sliding disintegration. (*a*) Sequence of sliding in 1 mM Mg-ATP taken every 0.14 s; (*b*) in 0.02 mM Mg-ATP taken every 1 s. Bar, 5 μm.

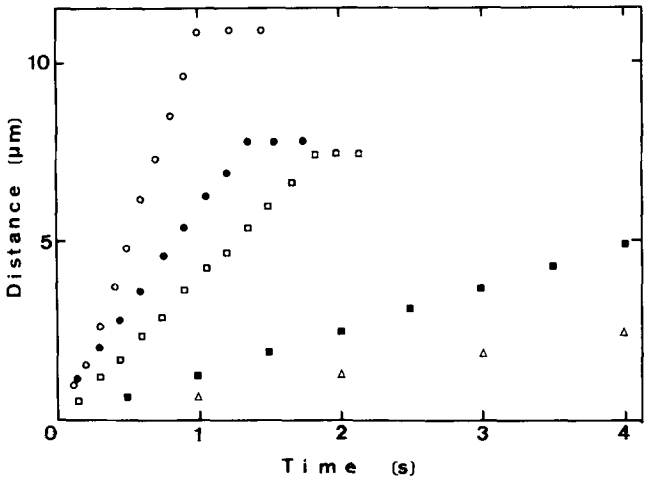

Figure 4. Plot of sliding distance against time. Mg-ATP concentrations: 1 mM (○); 0.1 mM (●); 0.05 mM (□); 0.02 mM (■); 0.005 mM (△). Wild-type axonemes.

for both wild-type and *oda38* axonemes. The results obtained with and without Ca^{2+} were identical within experimental errors over the range of Mg-ATP concentrations between 0.02 and 1 mM (Table II). Therefore we concluded that the sliding movement in the proteolysed axonemes was not sensitive to Ca^{2+}. This result is consistent with studies on axonemes of *Paramecium* and mussel gill cilia, which also showed that microtubule sliding was insensitive to the presence or absence of calcium ion although the movement of these axonemes is regulated by this ion (23, 33).

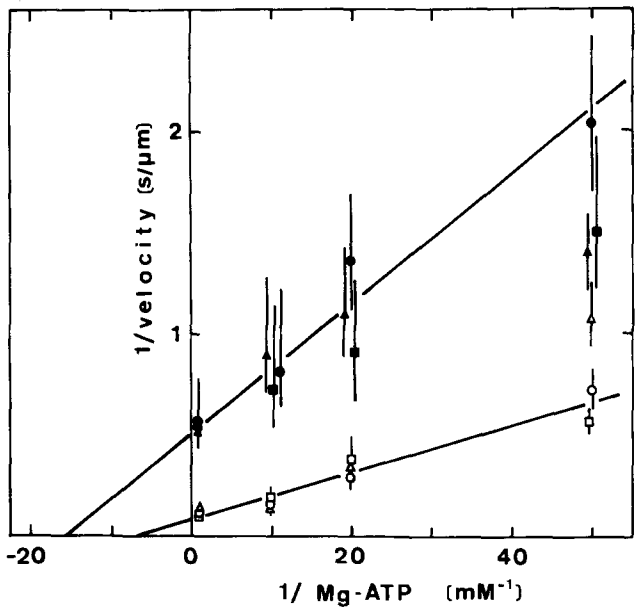

Figure 5. Double reciprocal plot of the sliding velocity of microtubules against Mg-ATP concentration. Open symbols, wild-type axonemes; closed symbols, *oda38* axonemes. Different symbols represent results obtained with different preparations of axonemes. Each data point is an average of ~20 measurements. Vertical bars represent deviations of the plot calculated from the standard deviation of the measured sliding velocities. Linear regression lines were drawn for the three sets of mean values obtained at 0.05, 0.1, and 1.0 mM Mg-ATP; data at 0.02 mM Mg-ATP were omitted because of the large scatter.

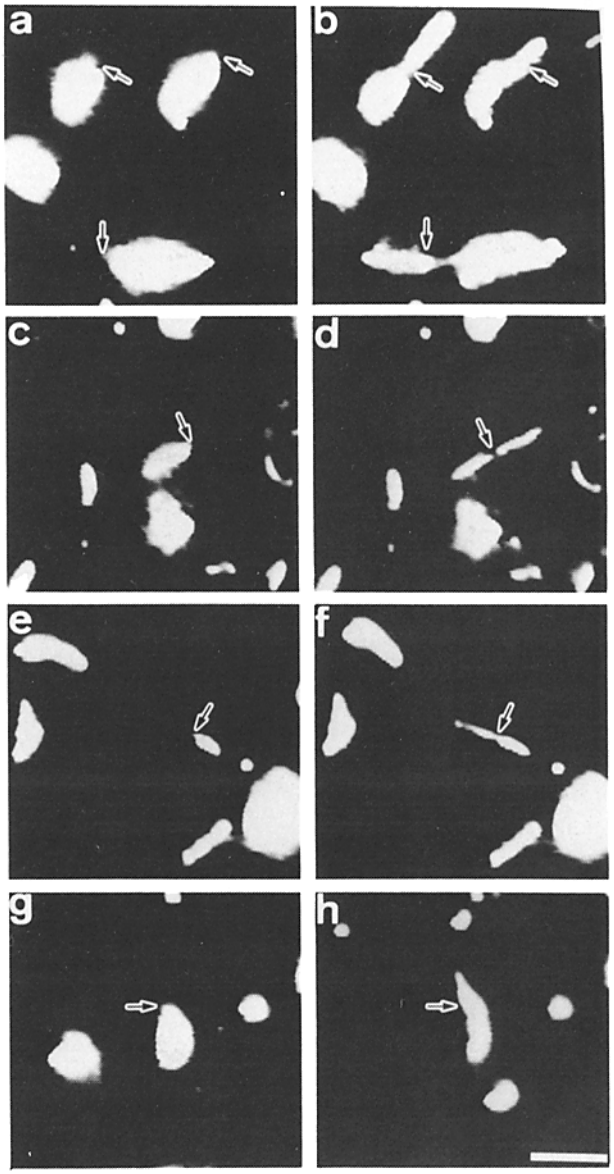

Figure 6. Sliding disintegration of mutant axonemes lacking outer or inner dynein arms in 0.1 mM Mg-ATP. (*a* and *b*) *oda38*; (*c* and *d*) *pf13A*; (*e* and *f*) *pf22*; (*g* and *h*) *pf23*. Videotaped images of axoneme fragments before (*a*, *c*, *e*, and *g*) and after (*b*, *d*, *f*, and *h*) sliding disintegration. Arrows indicate tips of axonemes that undergo sliding disintegration. Bar, 5 μm.

Microtubule Sliding in Nonmotile Axonemes

Nonmotile *Chlamydomonas* mutants lacking the outer (*pf-13A*, *pf22*) or the inner dynein arms (*pf23*) have been isolated (14). We examined these axonemes as to whether their microtubules could actively slide apart upon perfusion with ATP and protease. The gametes of *pf13A*, *pf22*, and *pf23* under our cultivating conditions displayed only irregular twitching movements of the flagella. Cell models of these mutants, prepared by the method previously reported (18), were completely nonmotile under reactivating conditions. We prepared axonemes from these gametes and perfused them with a solution containing nagarse and 0.1 mM Mg-ATP. This concentration of Mg-ATP was used because a higher one reduced the number of disintegrated axonemes;

Table II. Effect of Calcium Ion on the Velocity of Microtubule Sliding

Mg-ATP concentration	Sliding velocity (μm/s)			
	Wild type		*oda38*	
	$-Ca^{2+}$	pCa 5	$-Ca^{2+}$	pCa 5
mM				
0.02	1.6 ± 0.7	1.9 ± 0.9	0.6 ± 0.1	0.6 ± 0.2
0.05	3.3 ± 0.5	3.5 ± 0.6	1.2 ± 0.5	1.1 ± 0.6
0.10	4.8 ± 0.7	4.2 ± 0.5	1.3 ± 0.5	1.4 ± 0.6
1.00	9.2 ± 1.0	9.2 ± 1.0	1.7 ± 0.5	1.8 ± 0.5

Each value is an average of 15–23 measurements.

Table III. Sliding Velocity in Mutant Axonemes

Strain	Motility	Missing dynein arm	Sliding velocity at 0.1 mM Mg-ATP
			μm/s
Wild type	+	None	6.5 ± 1.4 (n = 25)
oda38	+	Outer	1.2 ± 0.2 (n = 21)
pf13A	−	Outer	0.8 ± 0.2 (n = 9)
pf22	−	Outer	0.2 − 0.3 (n = 2)
pf23	−	Inner	0.9 − 1.1 (n = 2)

at a lower concentration, the sliding velocity was so low that measurement was difficult.

Sliding disintegration was relatively easily observed in *pf13A* axonemes, with an average velocity close to that of *oda38* (Fig. 6, *c* and *d*; Table III). However, the other outer arm–deficient mutant *pf22* only very rarely displayed sliding and the sliding velocity obtained from two recordings was much smaller than that observed in *oda38* or *pf13A* axonemes (Fig. 6, *e* and *f*). Sliding disintegration in the axoneme of the inner arm–deficient mutant *pf23* was also a rare event; only about 20% of the total axonemal fragments showed signs of sliding disintegration in the usual experiment (Fig. 6, *g* and *h*). The sliding velocity obtained from two recordings was close to those for *oda38* and *pf13A* axonemes (Table III).

Discussion

Using an efficient method to induce sliding disintegration in *Chlamydomonas* axonemes, we measured the sliding velocity of microtubules in the wild-type and several types of dynein arm–deficient axonemes. Measurements at different Mg-ATP concentrations gave the maximal sliding velocity and the apparent Michaelis constant (K_m) of 13.2 μm/s and 158 μM for the wild type and 2.0 μm/s and 64 μM for a mutant lacking the outer dynein arm (*oda38*), respectively. The values of K_m agreed well with those obtained from beat frequencies of axonemes: 100 μM (wild-type) and 60 μM (*oda38*) (18).

The maximal sliding velocities obtained in this study do not agree with those estimated in beating axonemes. Brokaw and Luck (6), in their analysis of the waveform of wild-type flagella, determined the mean frequency to be 63.3 Hz and mean sliding velocity to be 340 rad/s. As the center-to-center distance between two outer doublet microtubules is ~80 nm, this would mean that the maximal sliding velocity is ~27 μm/s. In Nonidet-extracted axonemes, the maximal beat frequency was between 40 and 50 Hz in reactivation solutions used in this study (data not shown). If we assume that the reactivated waveform does not differ greatly from the in vivo pattern, these results should indicate that the sliding velocity of microtubules is 17–21 μm/s in the reactivated axonemes. These values are significantly larger than the 13.2 μm/s obtained in the present study. The disagreement was somewhat surprising because, in sea urchin sperm axonemes, the sliding velocities of microtubules measured in proteolysed axonemes have been shown to agree with the maximal sliding velocity estimated in beating axonemes in the same concentration of Mg-ATP (31).

The disagreement between sliding velocities in beating axonemes and disintegrating ones is still more pronounced in *oda38*. Nonidet-extracted *oda38* axonemes beat in a reactivation solution with a maximal frequency and a principal bend angle reduced to 1/2 and 2/3, respectively, of those of the wild-type axonemes. From these values we have estimated that the maximal sliding rate of microtubules in this mutant axoneme would be ~1/3 of that in the wild-type axoneme (18). This estimation was confirmed by a recent analysis of flagellar waveforms in live cells (Brokaw, C. J., and R. Kamiya, manuscript in preparation). In the present study, however, the maximal sliding velocity in *oda38* axonemes was ~1/6 of that of the wild-type axonemes.

The reason for the lower sliding velocities in disintegrating axonemes is not understood at present. One possibility is that proteolytic digestion destroyed some axonemal components responsible for the higher sliding velocity in intact axonemes. Since we obtained reproducible values of sliding velocity with different preparations of axonemes or with different protease solutions, it seems unlikely that proteolysis simply decreased the number of active dynein arms; if this were the case, the number of active dynein arms would have changed greatly from one experiment to another and the results would have shown much greater variation. However, it is possible that the digestion to the point of permitting sliding altered the nature of some or all of the dynein arms, and these modified dynein arms determined the over-all sliding velocity. Still another possibility is that microtubules in *Chlamydomonas* axonemes may be organized in such a way that they can slide faster when working cooperatively in beating axonemes than when moving separately in proteolysed axonemes.

Although the above disagreement remains to be resolved, the present data on *oda38* have shown that the sliding velocity produced by the inner arm alone is not simply half of that produced by the inner and outer arms working together. This differs from the case of the sea urchin sperm axonemes, in which depletion of the outer arms has been reported to result in an ~50% reduction of the sliding velocity, both in beating and disintegrating axonemes (8, 40). Because of this, we have been inclined to think that the inner and outer arms are functionally equivalent in sea urchin sperm axonemes. In *Chlamydomonas*, however, the inner and outer arms appear to be different, at least quantitatively.

We have shown that nonmotile axonemes from mutants lacking either outer (*pf13A*, *pf22*) or inner dynein arms (*pf23*) could display sliding disintegration. In *pf13A* axo-

nemes, sliding could be induced relatively easily and the sliding velocity was only slightly smaller than that of the motile *oda38* axonemes. Hence the inability of this kind of axoneme to beat may be due to some defects in the mechanism that converts the sliding movement into the organized movement of flagellar beating. In *pf22* axonemes, however, sliding was rarely observed, and the velocity was several-fold smaller than that of the *oda38* axonemes. This result suggests that the axoneme of this strain has a second intrinsic defect other than the lack of the outer arm, and this may directly interfere with the inner arm function.

Of special interest is the experiment with *pf23*, which is the only mutant known to lack the inner arm (14). Previous biochemical and structural studies have shown that the axoneme of this strain has an almost complete number of outer arms but only ~20% of the inner arms of the wild-type axoneme (14). The activity of Mg^{2+}-activated ATPase in this kind of axoneme has been reported to be ~60% of that of the wild-type axoneme; in contrast, the ATPase activity in *pf13A* is <10% of the wild-type activity (14). The present study showed that only a small fraction of *pf23* axonemes usually underwent sliding disintegration. Furthermore, despite the high ATPase activity present, the observed sliding velocity was close to those obtained with the outer-arm mutants, *oda38* or *pf13A*, which were much lower than the wild-type sliding velocity. This result raises two possibilities, the first that the axoneme of this particular mutant, besides lacking the inner arm, has some defects which prevent sliding disintegration, and the second and more interesting possibility that the outer arm in an axoneme may not be able to function well in the absence of the inner arm. Although ~20% of the *pf23* axonemal fragments displayed sliding disintegration in our experiment, it is still not certain whether the outer arm can function at all in the absolute absence of the inner arm, because a small number of inner arms must be present in the axonemes of this relatively leaky mutant (14).

Other mutants must be studied to come to any definite conclusions. If the outer dynein arm proves to be generally unable to function in the absence of the inner arm, the two kinds of arms will have to be regarded as being of completely different natures. Our efficient method of inducing sliding disintegration in *Chlamydomonas* axonemes should facilitate the characterization of many kinds of dynein arm mutants and thereby contribute to the understanding of the inner- and outer-dynein arm functions.

We thank Sho Asakura and Etsuko Hasegawa (Nagoya University) for discussion and David Luck (The Rockefeller University) for the gift of pf mutants.

This work was supported by grants-in-aid for scientific research from the Ministry of Education, Science and Culture of Japan.

Received for publication 28 March 1986, and in revised form 26 June 1986.

References

1. Allen, R. D. 1968. A reinvestigation of cross-sections of cilia. *J. Cell Biol.* 37:825–831.

2. Barman, T. E. 1969. *Enzyme Handbook II.* Springer-Verlag, Berlin. 631–632.

3. Bessen, M., R. B. Fay, and G. B. Witman. 1980. Calcium control of waveform in isolated flagellar axonemes of *Chlamydomonas*. *J. Cell Biol.* 86:446–455.

4. Bradford, M. M. 1976. A rapid and sensitive method for the quantitation of microgram quantities of protein utilizing the principle of protein-dye binding. *Anal. Biochem.* 72:248–254.

5. Brokaw, C. J. 1980. Elastase digestion of demembranated sperm flagella. *Science (Wash. DC).* 207:1365–1367.

6. Brokaw, C. J., and D. J. L. Luck. 1985. Bending patterns of *Chlamydomonas* flagella. III. A radial spoke head deficient mutant and a central pair deficient mutant. *Cell Motil.* 5:195–208.

7. Dirksen, E. R., and M. Zeira. 1981. Microtubule sliding in cilia of the rabbit trachea and oviduct. *Cell Motil.* 1:247–260.

8. Gibbons, B. H., and I. R. Gibbons. 1973. The effect of partial extraction of dynein arms on the movement of reactivated sea-urchin sperm. *J. Cell Sci.* 13:337–357.

9. Goodenough, U., and J. Heuser. 1984. Structural comparison of purified dynein proteins with *in situ* dynein arms. *J. Mol. Biol.* 180:1083–1118.

10. Goodenough, U. W., and J. E. Heuser. 1985. Substructure of inner dynein arms, radial spokes, and the central pair/projection complex of cilia and flagella. *J. Cell Biol.* 100:2008–2018.

11. Gorman, D. S., and R. R. Levine. 1965. Cytochrome F and plastocyanin: their sequence in the photosynthetic electron transport chain of *Chlamydomonas reinhardi*. *Proc. Natl. Acad. Sci. USA.* 54:1665–1669.

12. Hata, H., Y. Yano, and T. Miki-Noumura. 1979. ATP concentration dependency of the tubule-extrusion velocity from the axonemes. *Exp. Cell Res.* 122:416–419.

13. Hata, H., Y. Yano, T. Mohri, and T. Miki-Noumura. 1980. ATP driven tubule extrusion from axonemes without outer dynein arms of sea-urchin sperm flagella. *J. Cell Sci.* 41:331–340.

14. Huang, B., G. Piperno, and D. J. L. Luck. 1979. Paralyzed flagella mutants of *Chlamydomonas reinhardtii*: defective for axonemal doublet microtubule arms. *J. Biol. Chem.* 254:3091–3099.

15. Hyams, J. S., and G. G. Borisy. 1978. Isolated flagellar apparatus of *Chlamydomonas*: characterization of forward swimming and alteration of waveform and reversal of motion by calcium ions in vitro. *J. Cell Sci.* 33:235–253.

16. Kamimura, S., and K. Takahashi. 1981. Direct measurement of the force of microtubule sliding in flagella. *Nature (Lond.).* 293:566–568.

17. Kamiya, R. 1982. Extrusion and rotation of the central-pair microtubules in detergent-treated Chlamydomonas flagella. *Cell Motil. (Suppl.)* 1:169–173.

18. Kamiya, R., and M. Okamoto. 1985. A mutant of *Chlamydomonas reinhardtii* that lacks the flagellar outer dynein arm but can swim. *J. Cell Sci.* 74:181–191.

19. Kamiya, R., and G. B. Witman. 1984. Submicromolar levels of calcium control the balance of beating between the two flagella in demembranated models of *Chlamydomonas*. *J. Cell Biol.* 98:97–107.

20. Lindemann, C. B., and I. R. Gibbons. 1975. Adenosine triphosphate–induced motility and sliding of filaments in mammalian sperm extracted with Triton X-100. *J. Cell Biol.* 65:147–162.

21. Luck, D. J. L., G. Piperno, Z. Ramanis, and B. Huang. 1977. Flagellar mutants of *Chlamydomonas*: studies of radial spoke-defective strains by dikaryon and revertant analysis. *Proc. Natl. Acad. Sci. USA.* 74:3456–3460.

22. Mitchell, D. R., and J. L. Rosenbaum. 1985. A motile *Chlamydomonas* flagellar mutant that lacks outer dynein arms. *J. Cell Biol.* 100:1228–1234.

23. Mogami, Y., and K. Takahashi. 1983. Calcium and microtubule sliding in ciliary axonemes isolated from *Paramecium caudatum*. *J. Cell Sci.* 61:107–121.

24. Omoto, C. K., and C. J. Brokaw. 1985. Bending patterns of *Chlamydomonas* flagella. II. Calcium effects on reactivated *Chlamydomonas* flagella. *Cell Motil.* 5:53–60.

25. Piperno, G., and D. J. L. Luck. 1979. Axonemal adenosine triphosphatases from flagella of *Chlamydomonas reinhardtii*: purification of two dyneins. *J. Biol. Chem.* 254:3084–3090.

26. Piperno, G., and D. J. L. Luck. 1981. Inner arm dyneins from flagella of *Chlamydomonas reinhardtii*. *Cell.* 27:331–340.

27. Sale, W. S., and P. Satir. 1977. Direction of active sliding of microtubules in *Tetrahymena* cilia. *Proc. Natl. Acad. Sci. USA.* 74:2045–2049.

28. Summers, K. 1974. ATP-induced sliding of microtubules in bull sperm flagella. *J. Cell Biol.* 60:321–324.

29. Summers, K. E., and I. R. Gibbons. 1971. Adenosine triphosphate–induced sliding of tubules in trypsin-treated flagella of sea-urchin sperm. *Proc. Natl. Acad. Sci. USA.* 68:3092–3096.

30. Suzuki, M., and T. Miki-Noumura. 1985. Further properties of sliding disintegration of ciliary axonemes. *Cell Motil.* 5:142. (Abstr.)

31. Takahashi, K., C. Shingyoji, and S. Kamimura. 1982. Microtubule sliding in reactivated flagella. *In* Symposia of the Society for Experimental Biology XXXV, Prokaryotic and Eucaryotic Flagella. W. B. Amos, and J. G. Duckett, editors. Cambridge University Press. 159–177.

32. Tamm, S. L., and S. Tamm. 1984. Alternate patterns of doublet microtubule sliding in ATP-disintegrated macrocilia of the ctenophore. *Beroe. J. Cell Biol.* 99:1364–1371.

33. Walter, M. F., and P. Satir. 1979. Calcium does not inhibit active sliding of microtubules from mussel gill cilia. *Nature (Lond.).* 278:69–70.

34. Warner, F. D. 1970. New observations on flagellar fine structure: the relationship between matrix structure and the microtubule component of the axoneme. *J. Cell Biol.* 47:159–182.

35. Warner, F. D., and D. R. Mitchell. 1978. Structural conformation of ciliary dynein arms and the generation of sliding forces in *Tetrahymena* cilia. *J. Cell Biol.* 76:261–277.

36. Warner, F. D., and N. C. Zenetti. 1980. Properties of microtubule sliding disintegration in isolated *Tetrahymena* cilia. *J. Cell Biol.* 86:436–445.

37. Weaver, A., and R. Hard. 1983. Reactivation of isolated ciliary tufts: outer dynein arms do not contribute to beat frequency below 35 μM ATP. *J. Cell Biol.* 97(5, Pt. 2):197*a*. (Abstr.)

38. Witman, G. B., J. Plummer, and G. Sander. 1978. *Chlamydomonas* flagellar mutants lacking radial spokes and central tubules. *J. Cell Biol.* 76:729–747.

39. Yano, Y., and T. Miki-Noumura. 1980. Sliding velocity between outer doublet microtubules of sea-urchin sperm axonemes. *J. Cell Sci.* 44:169–186.

40. Yano, Y., and T. Miki-Noumura. 1981. Recovery of sliding ability in arm-depleted flagellar axonemes after recombination with extracted dynein I. *J. Cell Sci.* 48:223–239.